CHEMISTRY
A EUROPEAN JOURNAL

An Os^{II}–Bisbipyridine–4-Picolinic Acid Complex Mediates the Biocatalytic Growth of Au Nanoparticles: Optical Detection of Glucose and Acetylcholine Esterase Inhibition

Yi Xiao, Valeri Pavlov, Bella Shlyahovsky, and Itamar Willner*[a]

Abstract: The complex Os^{II}–bisbipyridine–4-picolinic acid, $[Os(bpy)_2PyCO_2H]^{2+}$ (**1**), mediates the biocatalyzed growth of Au nanoparticles, Au NPs, and enables the spectroscopic assay of biocatalyzed transformations and enzyme inhibition by following the Au NP plasmon absorbance. In one system, $[Os(bpy)_2PyCO_2H]^{2+}$ mediates the biocatalyzed oxidation of glucose and the growth of Au NPs in the presence of glucose oxidase, GOx, $AuCl_4^-$, citrate and Au NP seeds. The mechanism of the Au NPs growth involves the oxidation of the $[Os(bpy)_2PyCO_2H]^{2+}$ complex by $AuCl_4^-$ to form $[Os(bpy)_2PyCO_2H]^{3+}$ and Au^I. The $[Os(bpy)_2PyCO_2H]^{3+}$ complex mediates the GOx biocatalyzed oxidation of glucose and the regeneration of the mediator **1**. Citrate reduces Au^I and enlarges the Au seeds by the catalytic deposition of gold on the Au NP seeds. In the second system, the enzyme acetylcholine esterase, AChE, is assayed by the catalytic growth of the Au NPs. The hydrolysis of acetylcholine (**2**) by AChE to choline is followed by the $[Os(bpy)_2PyCO_2H]^{3+}$ mediated oxidation of choline to betaine and the concomitant growth of the Au NPs. The mediated growth of the Au NPs is inhibited by 1,5-bis(4-allyldimethylammonium-phenyl)pentane-3-one dibromide (**3**). A competitive inhibition process was demonstrated (K_M = 0.13 mM, K_I = 2.6 μM) by following the growth of the Au NPs.

Keywords: enzymes · gold · inhibitors · nanotechnology · sensors

Introduction

Metal nanoparticles (NPs) are used as active components for the optical and electrical sensing of biorecognition processes.[1] For example, the interparticle plasmon interactions of Au NPs functionalized with nucleic acids were used to analyze DNA and to detect single base mismatches.[2] Electrochemical detection of DNA was accomplished by the use of nucleic acid-functionalized metal NPs as labels, that after dissolution enable the electrochemical detection of the released ions.[3] Similarly, nucleic acid-modified Au NPs were used as "weight labels" for the microgravimetric quartz crystal microbalance analysis of DNA.[4] The catalytic properties of metal NPs towards the deposition of metals were extensively used for the amplified biosensing of antigen–antibody complexes,[5] DNA hybridization processes[6] and aptamer–protein binding.[7] For example, the catalytic enlargement of Au NP-labeled DNA complexes between electrodes was used for the biosensing of DNA by conductivity measurements.[8] Also, the catalytic enlargement of Au NPs was recently applied for the optical detection of aptamer–protein interactions on surfaces.[7]

The integration of enzymes with metal NPs has attracted recent scientific interest.[9] We have reported on the reconstitution of an apo-enzyme on cofactor-functionalized Au NPs to yield an electrically contacted redox enzyme with electrode supports.[9b] A different approach to couple enzymes and metal NPs has involved the use of the biocatalysts for growing NPs, and using the growth process to identify the substrate, the enzyme activity, or the enzyme inhibition.[10–12] For example, the catalytic enlargement of Au NPs by the reduction of Au^{III} salts with NAD(P)H cofactors was reported, and the optical detection of NAD^+-dependent biocatalytic transformations was accomplished.[10] Similarly, the NADH-mediated growth of shaped Au NPs (in the form of dipods, tripods and tetrapods) was used to develop an optical biosensor for the detection of ethanol in the presence of the NAD^+/alcohol dehydrogenase system.[11] A related approach was recently applied to analyze tyrosinase-generated neurotransmitters and to follow tyrosinase activity.[12]

The activation of redox enzymes by transition-metal complexes that mediate electron transfer is a common practice

[a] Dr. Y. Xiao, Dr. V. Pavlov, B. Shlyahovsky, Prof. I. Willner
Institute of Chemistry, The Hebrew University of Jerusalem
Jerusalem 91904 (Israel)
Fax: (+972) 2-652-7715
E-mail: willnea@vms.huji.ac.il

DOI: 10.1002/chem.200400988

in electrochemical biosensor design.[13,14] Specifically, Os^{II}–polypyridine complexes were extensively applied to activate flavoenzymes such as glucose oxidase by providing electrical contact between the redox-center of the enzyme and the electrode support.[15] In the present study, we demonstrate the novel use of a transition-metal complex as an electron-transfer carrier between biocatalytic redox sites of enzymes and Au NPs. We reveal that electron transfer mediates the catalytic deposition of gold on Au-NP seeds and we apply the optical imaging of the NPs growth to analyze the oxidation of glucose and the inhibition of acetylcholine esterase. In fact, in contrast to previous studies that used the mediated electron transfer to yield electrical current and to develop amperometric biosensors,[15] the present system uses the mediated electron transfer to grow NPs, and this enables the optical assay of the respective bioprocesses. Besides the possible use of the NP growth for the optical imaging of sensing processes, the systems have an important fundamental interest, as they add a new facet for the synthesis of metallic NPs.

Results and Discussion

The first system that will be described includes Os^{II}–bisbipyridine–4-picolinic acid (**1**), $[Os(bpy)_2PyCO_2H]^{2+}$, mediated growth of Au NPs in the presence of $AuCl_4^-$, 1.5×10^{-3} M, citrate, 7.5×10^{-3} M, GOx, glucose, and Au NP seeds, 2–3 nm, 2.5×10^{-8} M, that act as catalysts for the growth of the Au NPs. Figure 1, curve a, shows the absorbance spectrum of the Au NPs formed after 10 minutes of reaction in the presence of 5.9×10^{-3} M glucose, when the system is under Ar. An intense plasmon absorbance band of the formed Au NPs is observed at 532 nm. Figure 1, curve b, shows the absorbance spectrum of the same experiment, when performed under air. Clearly, the Au NPs are also formed in this system, but the intensity of the plasmon band at $\lambda=532$ nm is about 30% lower, implying that oxygen results in the inhibition of the particle growth. Several control experiments and complementary experiments were performed to elucidate the mechanism of formation of the particles. Figure 1 curves c–g depicts the absorption spectra of the system upon the specific exclusion of the $AuCl_4^-$, in the absence of $[Os(bpy)_2PyCO_2H]^{2+}$, but in the presence of O_2, upon the exclusion of citrate from the system, and upon the exclusion of glucose or GOx from the system, respectively. The control experiments reveal that in none of these systems Au NPs are formed and that the effective formation of the Au NPs depends on the presence of all of the components in the system. The experiment where the Os^{II} complex is excluded from the system is particularly interesting. In the absence of the Os^{II} complex, the O_2-mediated oxidation of glucose by GOx proceeds to yield H_2O_2. Previous studies have suggested that H_2O_2 may act as a reducing agent for $AuCl_4^-$ to form Au NPs.[16] Nonetheless, under the present experimental conditions the H_2O_2-stimulated growth of the particles is excluded (cf. Figure 1, curve d). To understand the functions

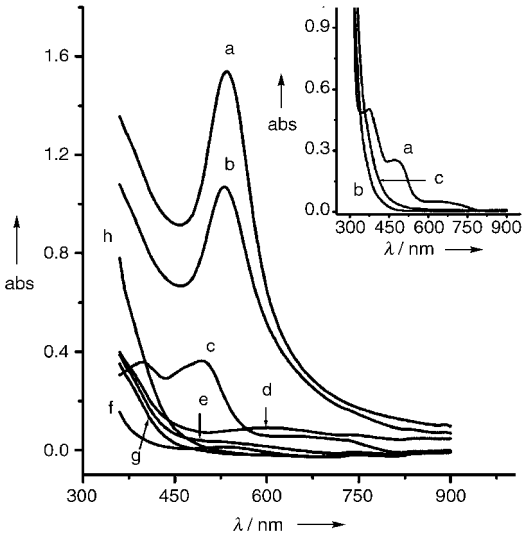

Figure 1. Absorbance spectra corresponding to: a) Au NPs formed in the glucose/GOx system in the presence of $[Os(bpy)_2PyCO_2H]^{2+}$, $AuCl_4^-$, citrate and 2.5×10^{-8} M Au-NP seeds under Ar; b) Au NPs generated in the glucose/GOx system in the presence of $[Os(bpy)_2PyCO_2H]^{2+}$, $AuCl_4^-$, citrate and Au NP seeds, under air; c) as described in b) but without $AuCl_4^-$; d) as described in b) but without $[Os(bpy)_2PyCO_2H]^{2+}$; e) as in b) but without citrate; f) and g) as described in b) but without glucose or GOx, respectively. The concentration of the respective components in the systems correspond to: 5.9×10^{-3} M glucose, 4.7 U mL^{-1} GOx, 1.5×10^{-3} M $AuCl_4^-$, 7.5×10^{-3} M citrate, 1×10^{-4} M $[Os(bpy)_2PyCO_2H]^{2+}$, 2.5×10^{-8} M Au-NP seeds. All spectra were recorded after a fixed time interval of 10 minutes. Inset: Absorbance spectra of: a) 1×10^{-4} M $[Os(bpy)_2PyCO_2H]^{2+}$; b) 1.5×10^{-3} M $AuCl_4^-$; c) 1×10^{-4} M $[Os(bpy)_2PyCO_2H]^{2+}$, after the addition of 1.5×10^{-3} M $AuCl_4^-$.

of the Os^{II} complex in the system, we added the complementary experiments shown in Figure 1, inset. An aqueous buffer system of the Os^{II} complex, 1×10^{-4} M, shows a spectrum consisting of a broad low absorbance band at about 670 nm and two bands of higher intensities at $\lambda=498$ and 400 nm (cf. inset, curve a). The $AuCl_4^-$ buffer solution includes an absorbance increase towards the UV region (see inset, curve b). Addition of $AuCl_4^-$ to the Os^{II} solution changes the structured Os^{II}-complex spectrum; this indicates that $AuCl_4^-$ oxidizes the Os^{II} complex to the Os^{III} species,[17] see Figure 1, inset, curve c. This set of experiments allows us to formulate the mechanism of Au NPs growth in the composite system (see Scheme 1). The Os^{II}-complex **1**, acts as electron-transfer mediator for the catalytic growth of the particles. The complex is reduced by $AuCl_4^-$ to form the Os^{III} complex that mediates the oxidation of the $FADH_2$ site in GOx formed upon the oxidation of glucose to gluconic acid; that is, the mediated biocatalytic oxidation of glucose generates continuous formation of the Os^{II} complex and the reduction of the $AuCl_4^-$ salt. Also, the control experiments allow us to define the detailed path for the growth of the NPs. Specifically, we see that added citrate, as co-reducing agent, is essential to stimulate the growth of the NPs. Thus, the enlargement of the Au NPs proceeds in two steps: In the first step, $AuCl_4^-$ is reduced by the Os^{II} complex to Au^I, as in Equation (1). In the second step, the citrate-mediated

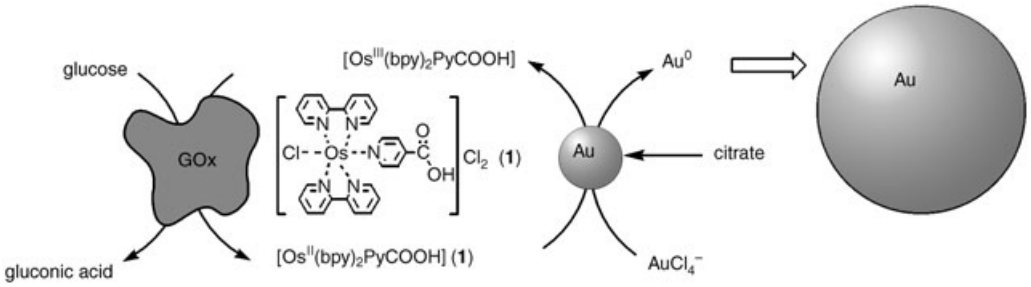

Scheme 1. Schematic $[Os(bpy)_2PyCO_2H]^{2+}$-mediated growth of the Au NPs in the glucose/GOx/citrate/Au NP seeds system.

$$2\,[Os^{II}(bpy)_2py\text{-}COOH] + AuCl_4^- \rightarrow 2\,[Os^{III}(bpy)_2py\text{-}COOH] + Au^I + 4Cl^- \quad (1)$$

reduction of Au^I in the presence of the Au NP seeds as catalytic sites takes place [Eq. (2)].

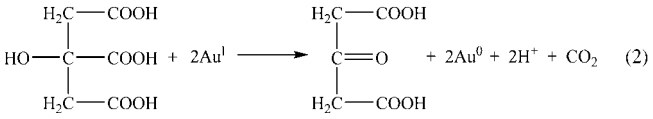

(2)

This stepwise formation of Au NPs with two reducing agents has already been reported for the NADH-mediated growth of Au NPs.[10] The elucidation of the mechanism for growing the Au NPs explains also the effect of the inert atmosphere on the growth of the NPs (cf. Figure 1 curve a vs b). The O_2-mediated oxidation of glucose to yield H_2O_2 competes with the Os^{II}-mediated growth of the particle. As a result, only a part of the enzyme (ca. 70%) is active in the mediated NPs growth, resulting in a lower growth efficiency under O_2 as compared to the inert atmosphere. These results indicate, however, that the formed H_2O_2 does not significantly affect the enhancement process of the NPs. Thus, most of the results that are presented here were performed under air. It should be noted that the concentration of the Au NP seeds is 2.5×10^{-8} M in all experiments shown in Figure 1. Although, the seeds gave a plasmon band at about 520 nm ($\varepsilon = 6.5\times10^5\ cm^{-1}M^{-1}$), they are not observed in the displayed spectra due to their low concentration.

Figure 2 shows the time-dependent absorbance of the GOx-generated Au NPs in the presence of two different concentrations of glucose. It can be seen that the absorbance of the Au NPs tends to saturate after a reaction time of about 30 minutes. After ≈10 minutes the absorbance values of the Au NPs reach about 50% of the saturation value; thus all biosensing experiments followed the formation of the Au NPs after a time interval of 10 minutes.

Figure 3 shows the absorbance spectra of the Au NPs formed in the system within a fixed time-interval of 10 minutes, upon introducing into the system different concentrations of glucose under air. The plasmon bands of the Au

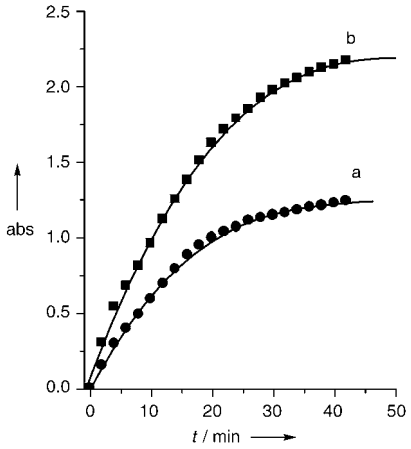

Figure 2. Time-dependent absorbance changes ($\lambda = 530$ nm) of the Au NPs generated in the system that included 2.5×10^{-8} M Au-NP seeds, 1×10^{-4} M $[Os(bpy)_2PyCO_2H]^{2+}$, 4.7 U mL^{-1} GOx, 1.5×10^{-3} M $AuCl_4^-$, 7.5×10^{-3} M citrate and different concentrations of glucose: a) 1.5×10^{-3} M, b) 3×10^{-3} M.

NPs are intensified and slightly red-shifted as the concentrations of glucose in the system increase. Thus, the Au NPs in the system increase in their dimensions as the concentration of glucose is increased. This combination is nicely supported by complementary TEM experiments. Figure 4a and b shows the image of the Au NPs formed in the system upon reaction with high (5.9×10^{-3} M) and low (7.4×10^{-5} M) concentrations of glucose for 10 minutes, respectively (note that the Au NP seeds have a diameter of 2–3 nm). At high concentrations of glucose, particles exhibiting dimensions of 90 to 110 nm are observed. For the lower concentration of glucose substantially smaller particles are observed, with diameters 10 to 30 nm, consistent with the spectral results. Figure 3, inset, curve a, shows the derived calibration curve, corresponding to the absorbance changes of the system upon analyzing different concentrations of glucose. For comparison, we depict also the derived calibration curve under an inert atmosphere, Figure 3, inset, curve b, to emphasize that the catalytic growth of the Au NPs is more efficient in the absence of O_2 from the reasons discussed above. The detection limit for analysis of glucose is about 7×10^{-5} M, a value comparable to the electrochemical sensing of glucose.

The successful use of the Os^{II}–bisbipyridine–4-picolinic acid (**1**) mediated growth of Au NPs for the optical detec-

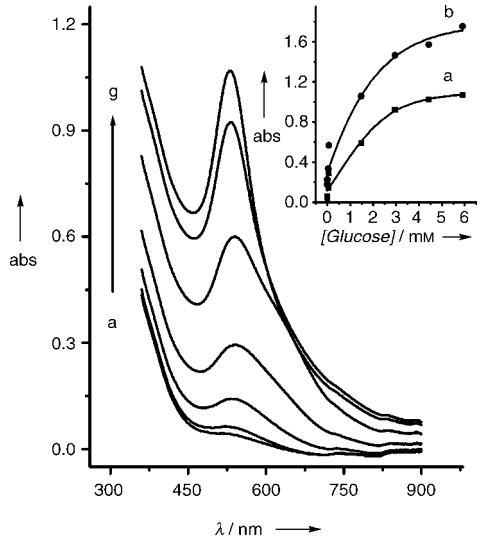

Figure 3. Absorbance spectra of the Au NPs formed in the system consisting of 4.7 U mL^{-1} GOx, 1×10^{-4} M $[Os(bpy)_2PyCO_2H]^{2+}$, 1.5×10^{-3} M $AuCl_4^-$, 7.5×10^{-3} M citrate, 2.5×10^{-8} M Au NP seeds, in the presence of different concentrations of glucose: a) 0 M, b) 7.4×10^{-5} M, c) 3.7×10^{-4} M, d) 7.4×10^{-4} M, e) 1.5×10^{-3} M, f) 3.0×10^{-3} M, g) 4.4×10^{-3} M. Spectra recorded under air after a time-interval of 10 minutes. Inset: calibration curve corresponding to the absorbance at $\lambda=530$ nm of the Au NPs formed in the presence of different concentrations of glucose: a) under air, b) under Ar.

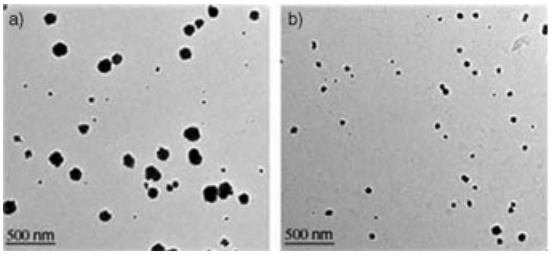

Figure 4. TEM images of: a) the Au NPs formed in the glucose/GOx system described in the caption of Figure 1, b) by using 5.9×10^{-3} M glucose and growth time-intervals of 10 minutes; b) as described in a) but 7.4×10^{-5} M glucose with 10 min growth time.

tion of glucose, suggests that the concept could be generalized for analyzing the substrates of other flavoenzymes such as lactate oxidase, choline oxidase, cholesterol oxidase or bilirubin oxidase. We decided, however, to apply the method to follow a biocatalytic process of higher complexity, namely the biocatalytic hydrolysis of acetylcholine by acetylcholine esterase, AChE, followed by biocatalytic oxidation of choline to betaine by choline oxidase. We attempted to characterize this enzyme cascade by the Os^{II}-mediated catalytic growth of the Au NPs and to follow the inhibition of the process in the presence of AChE inhibitors. Besides the fundamental interest of such assembly that follows a biocatalytic cascade by the NPs enlargement, the development of a system for sensing of AChE inhibitors could be of interest for analyzing chemical warfare, and could demonstrate the use of nanotechnology for homeland security applications.

Acetylcholine is a central neurotransmitter and its hydrolysis by acetylcholine esterase, AChE, is the main regulating process of the neural response system.[18] The inhibition of AChE, for example, by nerve gases leads to perturbations in nerve conduction process and the rapid paralysis of vital functions of the living system.[19] Different methods to sense the activity of AChE and to follow its inhibition were developed.[20] The most common method involves the activation of the enzyme cascade where AChE hydrolyses acetylcholine to choline and acetate. The subsequent O_2-mediated oxidation of choline in the presence of the flavoenzyme choline oxidase, ChOx, yields betaine and H_2O_2. The generated H_2O_2 activates horseradish peroxidase, HRP, towards the oxidation of organic substrates that enable the colorimetric[21] or electrochemical[22] detection of the primary AChE activity. Recently, CdS-semiconductor nanoparticles were coupled with AChE to yield a hybrid system that enable the photoelectrochemical detection of AChE activity and the inhibition of the enzyme.[23] In this system, thioacetylcholine was used as the substrate of the enzyme. Upon hydrolysis of the substrate, thiocholine, which shows electron-donor properties, was formed. The CdS–AChE hybrid system was immobilized on an Au electrode and upon the photoexcitation of the semiconductor NPs the conduction-band electrons were transferred to the electrode while thiocholine was oxidized by the valence-band holes. These processes gave rise to a photocurrent which followed the AChE activity. Upon inhibition of the enzyme the photocurrent in the system was blocked.

Realizing that Os^{II} complex **1** mediates the formation of Au NPs, while activating the oxidative paths of flavoenzymes, we decided to develop an assay to follow the activity and the inhibition of AChE by following the formation or the blocking of the formation of Au NPs, respectively, Scheme 2. In this system, the AChE hydrolyses acetylcholine (**2**), to choline and acetate. The Os^{II} complex present in the system in a catalytic amount is oxidized by $AuCl_4^-$, and the Os^{III} complex mediates the oxidation of choline to betaine in the presence of ChOx. The continuous regeneration of the Os^{III} complex by $AuCl_4^-$ leads to the enlargement of the Au seeds and to the formation of the Au NPs by a process analogous to that discussed for the GOx system. Note, that the enlargement of the Au NPs is controlled by the content of the choline in the system, and this is controlled by the efficiency of hydrolysis of acetylcholine by AChE. Thus, upon the inhibition of the enzyme, for example, by nerve gases, the enlargement of the Au NP seeds is anticipated to be slowed down and eventually blocked.

The system consists of AChE, acetylcholine chloride (**2**), ChOx, $AuCl_4^-$, 1.5×10^{-3} M, the Os^{II} complex, 1×10^{-4} M, citrate, 7.5×10^{-3} M, and Au NP seeds, 2.5×10^{-8} M. Figure 5, curve a, shows the absorption spectrum observed after 10 minutes in the presence of acetylcholine, 7.6×10^{-5} M, and AChE, 1.59 U mL^{-1}, and ChOx, 0.49 U mL^{-1}. The plasmon band at $\lambda=550$ nm indicates the formation of Au NPs in the system. In a control experiment, where the Os^{II} complex was excluded from the system, a substantially smaller ab-

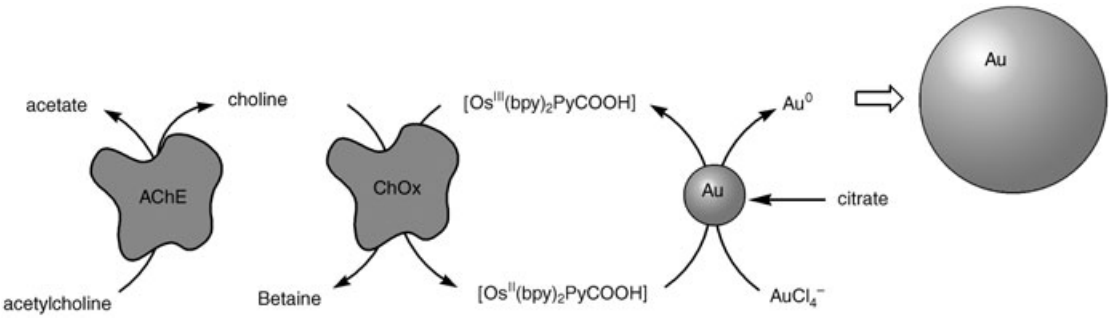

Scheme 2. Schematic $[Os(bpy)_2PyCO_2H]^{2+}$-mediated growth of the Au NPs in the AChE/ChOx/acetylcholine/citrate/Au seeds NP system.

sorbance band, which corresponds to Au NPs, is observed, see Figure 5, curve b. This inefficient formation of Au NPs in the absence of the Os^{II} complex is attributed to the progress of the O_2-mediated oxidation of choline by ChOx. The generated H_2O_2 acts then as a reducing agent that reduces $AuCl_4^-$ to the Au NPs. Indeed, in a further control experiment the latter inefficient formation of the Au NPs was totally blocked under an inert argon environment. In turn, the very efficient formation of Au NPs was observed under an inert atmosphere in the system that included the Os^{II} complex (a 25% enhancement in the production of the Au NPs was observed in the system which includes the Os^{II} complex under Ar as compared to the system under air). In additional control experiments, exclusion of either AChE or citrate or acetylcholine, no formation of Au NPs was detected in the systems, Figure 5 curves c–e, respectively. Also, in the absence of the Au NP seeds no enlarged Au NPs were formed. These results allow us to formulate the mechanism that leads to the formation of the Au NPs, Scheme 2. The Os^{III} complex formed upon the reduction of $AuCl_4^-$ oxidizes the redox center of ChOx, and mediates the oxidation of choline to betaine. The formation of the Au NPs requires the coexistence of two reducing agents in the system, the Os^{II} complex and citrate, and Au NP seeds that act as catalysts for the formation of the enlarged particles. The enlargement of the Au NPs proceeds in two steps: in the primary step, the Os^{II} complex reduces the $AuCl_4^-$ salt to Au^I [Eq. (1)], ($E_{Os^{II}/Os^{III}} = 268$ mV vs SCE). In the second step, citrate reduces Au^I to yield the enlarged particles. TEM analyses confirm the formation of the enlarged Au NPs, and while the Au NP seeds have a diameter of 2 to 3 nm, the enlarged particles formed after 10 minutes in the presence of acetylcholine, 2.4×10^{-4} M, have an average diameter of about 90 nm.

Figure 6A shows the absorbance spectra of the resulting enlarged Au NPs formed in the presence of a fixed concentration of enzyme, 1.59 U mL^{-1}, and variable concentrations of acetylcholine. As the concentrations of acetylcholine increase, the plasmon bands of the Au NPs intensify; this indicates the formation of larger particles. These results are consistent with the fact that as the concentrations of acetylcholine increase elevated amounts of choline are produced in the system, and these enhance the Os^{III}-mediated ChOx oxidation of choline. The latter process accelerated the regeneration of the Os^{II} complex and the production of the enlarged Au NPs. Figure 6B shows the absorbance spectra of the resulting Au NPs in the presence of a fixed concentration of acetylcholine, 3.8×10^{-5} M, but using different amounts of AChE in the system. Clearly, as the amounts of AChE increase the absorbance bands of the resulting Au NPs are intensified. These results are consistent with the fact that as the concentration of AChE increases the amount of generated choline is elevated. As the concentration of the AChE increases the concentration of the product, choline, is higher, and thus, the Os^{III}-mediated oxidation of choline by ChOx, and the formation of the Au NPs are enhanced.

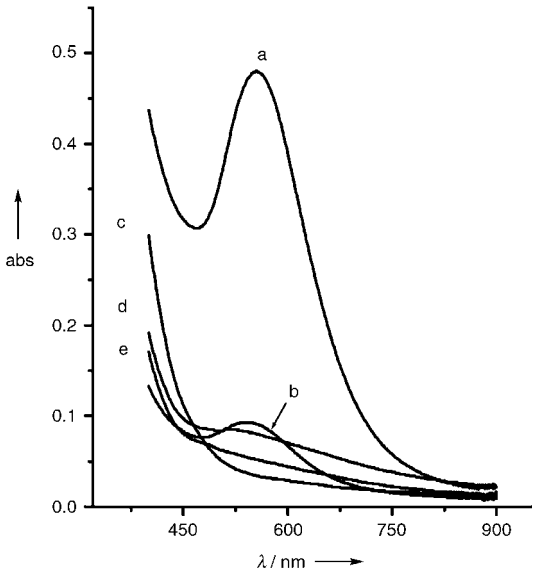

Figure 5. Absorbance spectra of a) The Au NPs generated in the system consisting of AChE (1.59 U mL^{-1})/ChOx (0.49 U mL^{-1})/acetylcholine (7.6×10^{-5} M), 1×10^{-4} M $[Os(bpy)_2PyCO_2H]^{2+}$, 1.5×10^{-3} M $AuCl_4^-$, 7.5×10^{-3} M citrate, 2.5×10^{-8} M Au-NP seeds, under air; b) as described in a) but without $[Os(bpy)_2PyCO_2H]^{2+}$; c)–e) as described in a) upon the exclusion of AChE, citrate or acetylcholine, respectively. All spectra were recorded after a fixed time-interval of 10 minutes.

Accordingly, we have examined the growth of the Au NPs by the composite system in the presence of different concentrations of 1,5-bis(4-allyldimethylammonium-phenyl)pen-

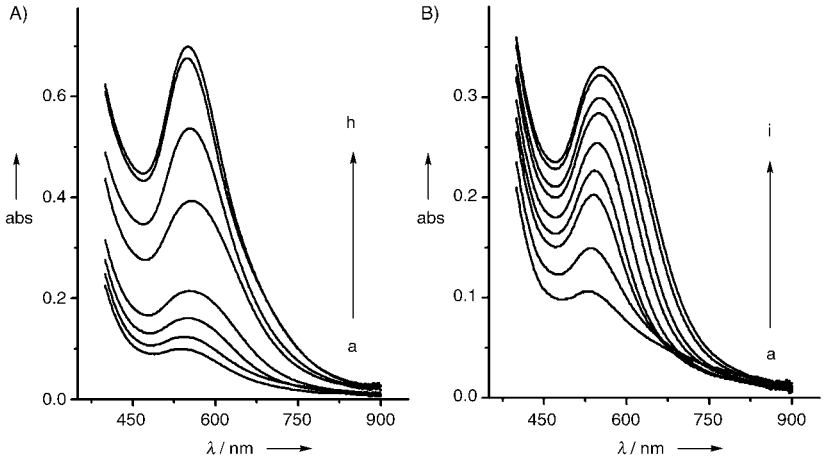

Figure 6. A) Absorbance spectra of the Au NPs formed in the system described in Figure 4a by using different concentrations of acetylcholine: a) 0 M, b) 7.6×10^{-6} M, c) 1.5×10^{-5} M, d) 2.3×10^{-5} M, e) 3.8×10^{-5} M, f) 7.6×10^{-5} M, g) 1.5×10^{-4} M, h) 2.4×10^{-4} M. B) Absorbance spectra of the Au NPs generated in the system described in Figure 4a by using a constant concentration of 3.8×10^{-5} M acetylcholine, and variable concentrations of AChE: a) 0 U mL^{-1}, b) 0.27 U mL^{-1}, c) 0.54 U mL^{-1}, d) 0.81 U mL^{-1}, e) 1.08 U mL^{-1}, f) 1.35 U mL^{-1}, g) 1.62 U mL^{-1}, h) 1.90 U mL^{-1}, i) 2.16 U mL^{-1}. For all systems the spectra were recorded after a fixed time-interval of 10 minutes under air.

AChE activity and its inhibition. The method seems to be very general and its further development in different directions seems obvious. The application of other transition-metal complexes, the growth of other metals, and the application of the method to sense other substrates (by using other flavoenzymes) or elucidate the activity of other enzyme cascades are reasonable directions to develop. Of particular interest would be the transformation of the solution-based analyses reported here into surface-confined assays. Such systems would establish handy optical biosensing strips. Furthermore, the mediated growth of the Au NPs on surfaces might be extended to related assays that use other readout signals such as conductivity or change in the frequency of piezoelectric crystals.

tane-3-one dibromide (**3**), which is used as a common inhibitor of AChE, and mimics the functions of nerve gases.[24] Figure 7 shows the absorption spectra of the resulting Au NPs in the system in the absence (curve a) of the inhibitor **3** and in the presence of increasing amounts of the inhibitor (curves b–d). As the concentration of the inhibitor increases, the absorbance of the resulting NPs decreases in its intensity, indicating the formation of smaller NPs. Indeed, TEM analyses confirm this conclusion, and while after 10 minutes of reactions, in the absence of the inhibitor, Au NPs with diameters corresponding to 90–100 nm are formed. In the presence of **3**, 7.6×10^{-6} M, substantially smaller particles are formed under the same conditions, exhibiting a diameter in the range of 15 to 35 nm. Realizing that the plasmon absorbance of the Au NP provides an optical signal that probes the enzyme activity, we analyzed the mechanism of inhibition by following the kinetics of Au NPs formation at different concentrations of the inhibitor, and variable concentrations of the substrate. The inset in Figure 7 shows the derived Lineweaver–Burk plots. From the shape of the plot, we conclude that a competitive inhibition mechanism is operative, and the values $K_I = 2.6$ μM and $K_M = 0.13$ mM are derived for the system. These values are in excellent agreement with the reported values of $K_M = 0.11$ mM and K_I (for **3**).[25]

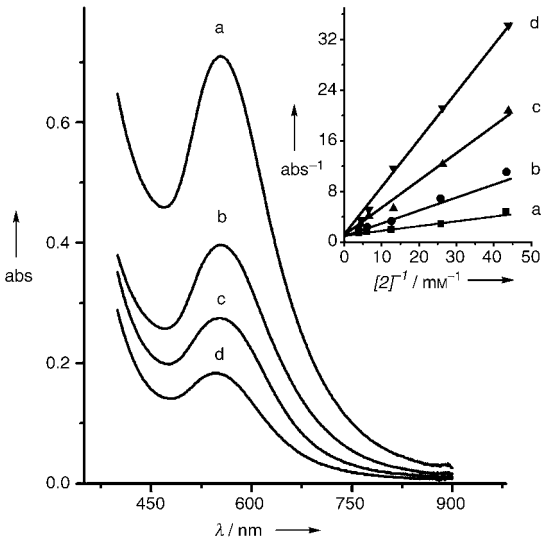

Figure 7. Absorbance spectra of the Au NPs formed in the system described in Figure 4a in the presence of 2.4×10^{-4} M acetylcholine, and variable concentrations of the inhibitor (**3**): a) 0 M, b) 7.6×10^{-7} M, c) 3.8×10^{-6} M, d) 7.6×10^{-6} M. Inset: Lineweaver–Burk plots corresponding to the inhibition of the Au NPs growth in the presence of different concentrations of **3**: a) 0 M, b) 7.6×10^{-7} M, c) 3.8×10^{-6} M, d) 7.6×10^{-6} M.

Conclusion

The present study has introduced a new method to couple the biocatalytic functions of flavoenzymes and the catalytic growth of Au NPs by the application of the Os^{II}–bisbipyridine–4-picolinic acid (**1**) as an electron transfer mediator. The growth of the Au NPs enabled us to optically follow biocatalytic reactions, and to sense glucose or to follow the

Experimental Section

Os^{II}–bisbipyridine–4-picolinic acid (**1**), $[Os(bpy)_2PyCO_2H]^{2+}$, was prepared according to literature procedures.[26]

Glucose assay: Variable concentrations of β-glucose (Sigma) in 0.1 M Tris buffer (80 μL, pH 7.4), 2.5 mM $AuCl_4^-$ (Aldrich) solution (800 μL), 0.33 mM Os^{II} complex (400 μL), 1 M trisodium citrate (Aldrich) (10 μL), 417 U mL^{-1} glucose oxidase from *Aspergillus niger* (Sigma) (15 μL) and 1.1×10^{-6} M of 2–3 nm aqueous gold NP seeds (30 μL) were mixed to give the final concentrations of $AuCl_4^-$, 1.5×10^{-3} M, Os^{II} complex, 1×10^{-4} M, trisodium citrate, 7.5×10^{-3} M, glucose oxidase, 4.7 U mL^{-1}, Au-NP seeds, 2.5×10^{-8} M. The mixture was incubated for 10 minutes at 35 °C and the absorbance spectra of the resulting solutions were measured.

Acetylcholine esterase assay: 0.1 M acetylcholine chloride (**2**) in 0.1 M Tris buffer (80 μL, pH 8.0) and the varied concentrations of AChE solution (from Electric Gel, Sigma) in 0.1 M Tris buffer (4 μL) were incubated at 35 °C for 15 min. Afterwards, 2.5 mM $AuCl_4^-$ solution (800 μL), 0.33 mM Os^{II} complex (400 μL), 1 M trisodium citrate (10 μL), 44 U mL^{-1} choline oxidase (ChOx) solution (from *Alcaligenes* species, Sigma) (15 μL) and 1.1×10^{-6} M of 2–3 nm aqueous Au-NP seeds (30 μL) were added to the original solution to yield the final concentrations of acetylcholine, 3.8×10^{-5} M, $AuCl_4^-$, 1.5×10^{-3} M, Os^{II} complex, 1×10^{-4} M, choline oxidase, 0.49 U mL^{-1}, and gold NP seeds, 2.5×10^{-8} M. The absorbance spectra of the resulting solutions were measured after the mixtures were incubated for 10 min at 35 °C.

Acetylcholine assay: The assay was performed by using the above-mentioned reaction mixture while adding 415 U mL^{-1} AChE solution (4 μL) to obtain the final concentration of 1.59 U mL^{-1}, and using variable concentrations of acetylcholine in the primary hydrolysis step.

Determination of the inhibition constant of 1,5-bis(4-allyldimethylammonium-phenyl)pentan-3-one dibromide (3): The determination was performed by the introduction of different concentrations of the inhibitor **3** to the above-mentioned AChE assay and performing the assay in the presence of different concentrations of acetylcholine for each concentration of the inhibitor **3**.

Acknowledgement

This study is supported by the German–Israeli Program (DIP).

[1] a) C. M. Niemeyer, *Angew. Chem.* **2001**, *113*, 4254–4287; *Angew. Chem. Int. Ed.* **2001**, *40*, 4128–4158; b) E. Katz, A. N. Shipway, I. Willner, in *Nanoparticles-From Theory to Applications* (Ed.: G. Schmid), Wiley-VCH, Weinheim, **2003**, Chapter 6, pp. 368–421; c) E. Katz, I. Willner, J. Wang, *Electroanalysis* **2004**, *16*, 19–44.
[2] a) J. J. Storhoff, R. Elghanian, R. C. Mucic, C. A. Mirkin, R. L. Letsinger, *J. Am. Chem. Soc.* **1998**, *120*, 1959–1964; b) J. J. Storhoff, C. A. Mirkin, *Chem. Rev.* **1999**, *99*, 1849–1862.
[3] J. Wang, D. Xu, A. N. Kawde, R. Polsky, *Anal. Chem.* **2001**, *73*, 5576–5581.
[4] a) F. Patolsky, K. T. Ranjit, A. Lichtenstein, I. Willner, *Chem. Commun.* **2000**, 1025–1026; b) Y. Weizmann, F. Patolsky, I. Willner, *Analyst* **2001**, *126*, 1502–1504; c) X. C. Zhou, S. J. O'Shea, S. F. Y. Li, *Chem. Commun.* **2000**, 953–954.
[5] a) O. O. Velev, E. W. Kaler, *Langmuir* **1999**, *15*, 3693–3698; b) Y. C. Cao, R. Jin, J.-M. Nam, C. S. Thaxton, C. A. Mirkin, *J. Am. Chem. Soc.* **2003**, *125*, 14676- 14677; c) K. Faulds, W. E. Smith, D. Graham, *Anal. Chem.* **2004**, *76*, 412–417.
[6] a) J. Wang, O. Rincon, R. Polsky, E. Dominguez, *Electrochem. Commun.* **2003**, *5*, 83–86; b) J.-M. Nam, C. S. Thaxton, C. A. Mirkin, *Science* **2003**, *301*, 1884–1886.
[7] V. Pavlov, Y. Xiao, B. Shlyahovsky, I. Willner, *J. Am. Chem. Soc.* **2004**, *126*, 11768–11769.
[8] S. J. Park, T. A. Taton, C. A. Mirkin, *Science* **2002**, *295*, 1503–1506.
[9] a) M. Zayats, R. Baron, I. Popv, I. Willner, *Nano Lett.* **2005**, *5*, 21–25; b) Y. Xiao, F. Patolsky, E. Katz, J. F. Hainfeld, I. Willner, *Science* **2003**, *299*, 1877–1881.
[10] Y. Xiao, V. Pavlov, S. Levine, T. Niazov, G. Markovitch, I. Willner, *Angew. Chem.* **2004**, *116*, 4619–4622; *Angew. Chem. Int. Ed.* **2004**, *43*, 4519–4522.
[11] Y. Xiao, B. Shlyahovsky, I. Popov, V. Pavlov, I. Willner, unpublished results.
[12] R. Baron, M. Zayats, I. Willner, *Anal. Chem.* in press.
[13] a) I. Willner, E. Katz, *Angew. Chem.* **2000**, *112*, 1230–1269; *Angew. Chem. Int. Ed.* **2000**, *39*, 1180–1218; b) A. Heller, *Acc. Chem. Res.* **1990**, *23*, 128–134; c) L. Hubermuller, M. Mosbach, W. Schuhmann, *Fresenius J. Anal. Chem.* **2000**, *366*, 560–568.
[14] A. Heller, *J. Phys. Chem.* **1992**, *96*, 3579–5980.
[15] B. A. Gregg, A. Heller, *J. Phys. Chem.* **1991**, *95*, 5976–5980.
[16] T. K. Sarma, D. Chowdhury, A. Paul, A. Chattopadhyay, *Chem. Commun.* **2002**, 1048–1049.
[17] a) G. M. Bryant, J. E. Ferguson, *Aust. J. Chem.* **1971**, *24*, 275–286; b) M. K. Nazeeruddin, S. M. Zakeeruddin, K. Kalyanasundaramk, *J. Phys. Chem.* **1993**, *97*, 9607–9612; c) M. I. J. Polson, S. L. Howell, A. H. Flood, A. K. Burrel, A. G. Blackman, K. C. Gordon, *Polyhedron* **2004**, *23*, 1427–1439.
[18] a) I. Wessler, C. J. Kirkpatrick, K. Racke, *Clin. Exp. Pharmacol. Physiol.* **1999**, *26*, 198–205; b) E. Perry, M. Walker, J. Grace, R. Perry, *Trends Neurosci.* **1999**, *22*, 273–280.
[19] a) J. Pauluhn, L. Machemer, G. Kimmerle, *Toxicology* **1987**, *46*, 177–190; b) J. G. Clement, *Fundam. Appl. Toxicol.* **1983**, *3*, 533–535.
[20] a) I. B. Wilson, in *Methods in Enzymology* (Eds.: S. P. Colowick, N. O. Kaplan), Academic Press, New York, **1955**; b) L. Alfonta, E. Katz, I. Willner, *Anal. Chem.* **2000**, *72*, 927–935; c) W. Liu, C. L. Tsou, *Biochim. Biophys. Acta* **1986**, *870*, 185–190.
[21] M. Zhou, C. Zhang, R. P. Haugland, *Proc. SPIE-Int. Soc. Opt. Eng.* **2000**, *3926*, 166–171.
[22] A. Riklin, I. Willner, *Anal. Chem.* **1995**, *67*, 4118–4126.
[23] V. Pardo-Yissar, E. Katz, J. Wasserman, I. Willner, *J. Am. Chem. Soc.* **2003**, *125*, 622–623.
[24] a) P. L. Dipatre, C. W. Mathes, L. L. Butcher, *J. Histochem. Cytochem.* **1993**, *41*, 129–135; b) J. L. Dupree, J. W. Bigbee, *J. Neurosci. Res.* **1994**, *39*, 567–575.
[25] C. Costagil, A. Galli, *Biochem. Pharmacol.* **1998**, *55*, 1733–1737.
[26] C. Danilowicz, E. Corton, F. Battaglini, *J. Electroanal. Chem.* **1998**, *445*, 89–94.

Received: September 28, 2004
Published online: February 24, 2005